Novel Cattail Fiber Composites - Converting Waste Biomass into Reinforcement for Composites

Md Shadhin
University of Manitoba
Mashiur Rahman (mashiur.rahman@umanitoba.ca)
University of Manitoba https://orcid.org/0000-0001-8355-0849
Raghavan Jayaraman
University of Manitoba
Danny Mann
University of Manitoba

Research Article

Keywords: Cattail fiber composite, Waste biomass, Nonwoven mat, VARTM, Compression molding, Natural fiber composite.

Posted Date: June 15th, 2021

DOI: https://doi.org/10.21203/rs.3.rs-593117/v1

Version of Record: A version of this preprint was published at Bioresources and Bioprocessing on October 13th, 2021. See the published version at https://doi.org/10.1186/s40643-021-00453-8.

Abstract

Vacuum Assisted Resin Transfer Molding (VARTM), used to manufacture medium to large sized composites for transportation industries, require non-woven mats. While non-woven glass mats used in these applications are optimized for resin impregnation and properties, such optimized mats for natural fibers are not available. In the current research, cattail fibers were extracted from plants (18–30% yield) using alkali retting and nonwoven cattail fiber mat was manufactured. The extracted fibers exhibited a normal distribution in diameter ($d_{avg.}$ = 32.1 µm) and the modulus and strength decreased with increase in diameter with average values of 19.1 GPa and 172.3 MPa, respectively. The cattail fiber composites were manufactured using non-woven mats, Stypol polyester resin, and VARTM (101 kPa) and compression molding pressures (260 and 560 kPa) and tested. Out-of-plane permeability changed with V_f of mats, which was influenced by areal density, thickness, and fiber packing in the mat. The cattail fibers reinforced the stypol resin significantly. The modulus and the strength increased with consolidation pressures due to increase in fiber volume fraction (V_f), with maximum values of 7.4 GPa and 48 MPa, demonstrating the utility of Cattail fibers from waste biomass as reinforcements.

Introduction

Polymer-matrix composites (PMC) are increasingly used in structural applications. PMC can be categorized as a particulate composite, a discontinuous / short fiber composite, or a continuous fiber composite. Continuous fiber composites are used in structural applications in the aerospace industry, such as fairings, vertical and horizontal stabilizers and fuselage, where meeting the desired properties is more significant than the cost. However, discontinuous fiber composites are usually used in semi-structural or non-structural applications such as doors, window frames, and automotive interior parts, where cost is the primary consideration (Campbell 2010; Mazumdar 2001).

Natural fiber reinforced composites (NFRC) are gaining interest due to renewability of natural fibers over synthetic fibers currently in use. The natural bast fibers (BFs), such as flax, kenaf, jute, hemp, and sisal are increasingly being investigated as environmentally friendly alternatives to glass fibers for engineering applications (Fahimian 2013; Nishino et. al. 2003; Karnani 1997; Oksman 2002; Wambua et. al. 2003; Wrobel et. al. 2012; Yan et. al. 2014). The mechanical properties of NFRC rely on the fiber properties, fiber geometry, fiber orientation, and fiber volume fraction (Lau et. al. 2018; Ho et. al. 2012).

Cattail (*Typha latifolia*) fiber is a waste biomass fiber which is easy to extract, using an alkaline solution, from their raw resources. Cattail fiber has several advantages over BFs, which include lower density (1.26 g/cm^3), abundant supply without any cost for growing them, and higher fiber yield (%) of about 40 to 60% (Mortazavi et al. 2009; The Canadian Encyclopedia n.d.; Chakma 2018, Rahman et al. 2020).

Unlike BFs that are grown as main crop in majority of the cases, cattails grow naturally in bog and fen, lacustrine marshes, prairie pothole marshes, roadside ditches, riverine marshes, tidal marshes, and becoming increasingly dominant wetland plants in North America (Shih & Finkelstein 2008). When

compared with other bast fibers, the chemical composition in cattail fiber is similar in terms of cellulosic content (Faruk et. al. 2012; Vetayasuporn 2007).

To the best knowledge of the authors, use of cattail fibers in composite applications have not been studied in the past. Hence, this research is focused on evaluating the suitability of cattail fibers for composite applications. Cattail fibers were extracted from the leaves and preformed to obtain a nonwoven mat. Composites were manufactured using these mats using VARTM and Compression molding. Mechanical properties of these composites were determined and evaluated to demonstrate the suitability of these fibers in composite applications.

Experimental Details

Materials

Green cattail plants were collected from the roadside ditches along the Provincial Highway 3 near Winnipeg, Canada in early October 2019 (Fig. 1 (a)). Aqueous KOH (Fisher Scientific, Ontario, Canada) was used for fiber extraction while acetic acid (Fisher Scientific, Ontario, Canada) was used for the neutralization of the fiber after extraction. Unsaturated polyester resin (Stypol 8086) was used as the thermoset polymer matrix (Composite Envisions LLC, Wausau, USA). It is a low-viscosity resin, which starts reacting with the addition of a curing initiator. The curing initiator chosen for this study was Luperox 224 (2,4-Pentanedione peroxide, Sigma Aldrich, Oakville, Ontario, Canada).

Extraction of Cattail Fibers and Manufacturing of non-woven mat

The steps involved in transformation of the Cattail leaves into fibers, non-woven mat and composites are shown schematically in Fig. 1(a - k).

Fiber extraction

The collected cattail leaves were dried at room temperature for 48 h and precut to 6–10 cm in length (Fig. 1(b)) and weighed. At the beginning, fiber extraction conditions were varied by varying temperature (70, 80 and 90°C), time (2, 3, and 4 h) and alkaline concentrations (1, 2, 5 and 10%). 90°C temperature and 4 h treatment in 5% KOH were chosen to be the optimal extraction condition based on the individuality of the extracted fiber (single fiber entity) and flexibility.

A stock solution of 5% (w/v) KOH was prepared and the required amount (250 g) of cattail leaves was added into it. Its temperature was controlled using water bath (capacity: 12–15 L) covered with a lid (Fig. 1 (c)). Once the fibers were separated and individualized, they were rinsed in cold distilled water and neutralized in 2% (v/v) acetic acid solution for 30 min, which were subsequently washed progressively in cold, hot, and cold distilled water and left for drying at room temperature (Fig. 1(d)). The above procedure was repeated for 30 extraction runs.

Manufacturing mat

The extracted cattail fibers (Fig. 1(e)) were individualised using a modified laboratory carding machine by passing them through a pair of spiked rollers of the carding machine while a combing operation was conducted during the pass by each spiked roller (Fig. 1(f)). While the spiked roller helped to individualize the entangled fibers obtained from extraction, the combing operation helped to orient the individual cattail fibers parallel to one another (Figs. 1(g) and (h)). After that, mat manufacturing was completed using a customized template designed for this study; it consisted of a metal platen (21.5cm x 21.5cm) covered by a paper board on the sides for the ease of thickness control while laying up individualized fibers. The fibers were dropped by hand into the mold to avoid preferential orientation. Once the fibers were laid, a metal platen with the same dimension was placed on the top of the mat and a dead weight of 3 kg (6 x 0.5 kg) was applied to compress the fiber bed (Fig. 1 (i)).

Composite Manufacturing

The composite was manufactured using a VARTM mold. STYPOL 8086 mixed with (2% - w/w) the LUPEROX 224 initiator was degassed and injected into the mat using vacuum. After impregnation under vacuum pressure (~ 101 kPa), the composite was allowed to cure overnight (24 hours) at room temperature. Additional mats were cured under various consolidation pressures to study the effect of pressure. The mats impregnated using the VARTM set-up, were removed from the mold, right after resin impregnation, and were compression molded in a hydraulic press under the chosen pressure. The impregnated mat was sandwiched between two release films, which were subsequently sandwiched between two metal plates and two silicone pads and subjected to pressures of 260 and 560 kPa, using a G50 H- 24-CLX hydraulic press manufactured by WABASH MPI, IN, USA. The composites were left in the press for 8–10 hours to cure at room temperature.

Fiber characterization

Fiber Yield

The fiber yield (%) was determined as the ratio of the oven-dried mass of the fibers extracted after chemical treatment to the oven-dried mass of the cattail plants before chemical treatment.

Single fiber tensile testing

The mechanical properties, i.e., tensile strength, modulus of elasticity, and strain at break (%) of cattail fiber were evaluated using an Instron Tensile Tester (Model# 5965, Sl#VS02075661, Norwood, USA) following the ASTM D3822 method. Single cattail fibers were bonded to a paper frame with a rectangular hole in the center. Before tensile testing, cattail fiber's diameter was measured using an image analyzer (Bioquant life science - Motic, BA310l, 2010). The length of the fiber inside the rectangular hole of the frame (i.e., 25 mm) acted as the gage length to measure the strain. After clamping the frame bonded with the fibers between the clamps of the Instron tester, the paper frame was cut at the center so that the

tension was applied only on the fiber. Tensile testing was done at a crosshead speed of 20 mm/min, using a 1 KN load cell.

Mat characterization

Thickness, areal density and V_f

The thickness of each nonwoven mat was measured using a caliper. For areal density (gsm – gram per square meter) measurement, the weight of the manufactured mat sample for a given area (21.5cm x 21.5cm) was recorded. The fiber volume fraction (V_f) in the nonwoven mat was determined using Eq. (I)

$$\text{Fiber volume fraction, Vf } (\%) = \frac{\text{W}}{\text{A . h . } \rho\text{f}} \text{ (I)}$$

where, W is weight of cattail mat, A is the area, h is the mat thickness, and ρ_f is the density of reinforcing fiber.

Out-of-plane permeability

Frazier Permeability Tester (manufactured by Fraizer Precision Instrument Co. Inc. Hagerstown, MD. U.S.A) was used in this study to determine the volumetric flow rate through a nonwoven mat following the ASTM D-737 method. Airflow rate through the thickness of a nonwoven mat of known area is adjusted to obtain a prescribed air pressure drop (equivalent to 0.5 inch of water) across the thickness. The out-of-plane permeability (i.e., through-the-thickness), k_z ,was calculated using Darcy's law in Eq. (II).

$$\text{kz} = \frac{\text{Q } \eta \text{ L}}{\text{A } \Delta\text{P}} \text{ (II)}$$

Where, Q = volumetric flow rate

η = viscosity of air = 1.81 x 10^{-5} Pa s

A = Area of the specimen perpendicular to flow direction = 0.003788 m^2

ΔP = Pressure difference and L = length of mat parallel to the flow direction.

Composite characterization

Testing

The mechanical properties of manufactured composite were determined using an MTS tensile testing machine with 30 KN Load cell and extensometer with 2 in gage length, following ASTM D3039. All samples were stored in the lab atmosphere after preparation until testing. The testing was done at a crosshead speed of 2 mm/min. Five samples were tested for each consolidation pressure. The tensile

modulus of manufactured mat composite was calculated from the slope of the stress-strain curve from the initial linear portion in the strain range of 0.1%.

Before tensile testing, composite panels were bonded with tabs to the gripped ends using a room temperature curing adhesive to avoid crushing the gripped ends while tensile testing. The tabs were manufactured using 4 plies of woven carbon epoxy prepregs. 127 mm long and 20 mm wide composite test specimens were cut from the panels bonded with tabs using Micro-Matic Precision Wafering Machine (manufactured by Micromech Mfg. Corp.). A slow feed rate of 10 mm/min was used to prevent excessive heat evolution during cutting and damaging the edges of test specimens. Edges of the prepared testing coupons were ground progressively using 80, 180, 240, 320, and 400 grit silicon carbide papers and polished further using alumina powder to remove any damage due to cutting.

Density and fiber volume fraction measurement

The density of the flax fibers, the Stypol resin, and the manufactured composites were measured using Helium Pycnometer (Model#UPY-32, UPY-32T; v-5.04 manufactured by Quantachrome INSTRUMENTS) according to ASTM D4892-89. The volume fraction of fibers (V_f) in composite was calculated using Eq. (III), assuming 100% dense composite.

$$\mathrm{Vf}\ \ (\%) = \frac{\rho \mathrm{c} - \rho \mathrm{m}}{\rho \mathrm{f} - \rho \mathrm{m}} \mathrm{x}\ 100 \ (\mathrm{III})$$

where, ρ_f, ρ_m, ρ_c are the density of the fiber, the resin, and the composite, respectively.

Scanning Electron Microscopy (SEM) analysis

The fractured surfaces of the composite specimens from the tensile test were examined in a scanning electron microscope (FEI Quanta 650 FEG ESEM from Thermo Fisher Company, USA) at an accelerating voltage of 10.0 kV. Prior to the SEM analysis, the fractured cattail composite specimens were coated with a thin layer of gold-palladium film (20 nm) using a Desk II Cold Sputter Etch Unit under the chamber pressure of 30 mTorr.

Results And Discussion

Fiber Extraction

The cattail plant leaves, the extracted fibers after drying, and the individualized fibers are shown in Fig. 2. Yield of Cattail fiber, extracted in this study using optimum conditions (90°C for 4 h), varied between 18–30% as shown in Fig. 3. Cattail plants were not grown in controlled environment in this study and collected from wetlands in Winnipeg. So, it is expected to have variations in the cattail plant cultivar collected from different locations, which is believed to be the reason of variation in the yield %. This fiber yield (%) is less than the previously reported cattail fiber yield (40%) (Hasan 2019), which is believed to be due to the use of green plant for the current study, whereas Hasan (2019) used mature dried plants.

Physical properties of Cattail Fibers

The length of the extracted cattail fiber depends on the cut length of leaves before extraction and the fiber length after extraction varied between 4 and 12 cm while the diameter varied between 13 and 53 µm exhibiting a normal distribution as shown in Fig. 4. The average fiber diameter is 32.1 µm and the average fiber length is 6.98 cm. While the diameter is smaller, the length is longer than hemp of flax or hemp fibers as shown in Table 1.

Table 1
Physical and mechanical properties of flax, hemp, and cattail fiber.

Parameters	Flax	Hemp	Cattail
Length (cm)	6.64 (2.3)	0.4–21 [a]	6.98 (1.2)
Diameter (µm)	80.2 (32.7)	138.3 (31.9) [a]	32.1 (8.6)
Density (gm/cm^3)	1.49 (0.004)	1.57 (0.003)	1.39 (0.005)
Tensile strength (MPa)	180.1 (126.1)	172.1 [a]	172.3 (99.3)
Modulus (GPa)	11.3 (10.7)	28.5 [a]	18.1 (9.7)
[a] Fahimian (2013)			

The experimental density value of cattail fiber and stypol resin are 1.39 gm/ cm^3 (SD = 0.005) and 1.16 g/cm^3 (SD = 0.001), respectively. The cattail fiber is lighter than and hemp fibers (see Table 1), which is believed to be due to the hollow structure of the cattail fiber (Rahman et al. 2020). The recorded density value of Stypol resin in this study (1.16 g/ cm^3) is lower than previously reported density value (1.3 gm/cm^3) of stypol resin (Fahimian 2013). This could be due to the difference in the amount of initiator as well as possible differences in resin batches.

A SEM image of cattail fiber is shown in Fig. 5. The rectangular calcium oxalate plates and pit areas (without oxalate plates) can be seen on the surface of the virgin cattail fibres. These plates lie along the fiber axis and their length and width are vary from location to location.

Mechanical properties of cattail fiber

The experimental tensile modulus (E_f) and tensile strength (σ_f) of virgin cattail fiber varied with fiber diameter as shown in Fig. 6(a) and 6(b), respectively. Tensile modulus (E_f) decreased with increase in fiber diameter (D_f). Similar trend was observed for tensile strength. This relationship is modeled by the empirical equation as shown in Eq. (IV and V). This trend is similar to that observed in flax fibers

(Shadhin 2021) and hemp fibers (Fahimian 2013). The tensile strength varied from 9 to 365 MPa (avg. = 172.3 ± 99.3) and tensile modulus varied from 3 to 40 GPa (avg. = 19.1 ± 9.6). Similar variations in tensile strength and modulus were reported for other bast fibers (Li et al. 2007; Joffea et al. 2003; Ali 2013; Ibrahim et al. 2018). The modulus and the strength of cattail fibers have been found to change with moisture content with a maximum after conditioning at 75.5% RH for 72 hours during which the fibers absorbed ~ 15% moisture (Shadhin 2021). The fibers used in this study were stored in lab atmosphere with a humidity of ~ 50–60%. It can be inferred from Table 1 that the tensile modulus of cattail fibers is higher than flax fibers but lower than that of hemp fibers. The tensile strength of cattail fibers is comparable to that of hemp and flax fibers. While specific strength (strength/density) is higher than hemp and flax fibers, the specific modulus (modulus/density) is in between that of hemp and flax fibers. These results suggest that the mass and properties of composites manufactured with cattail fibers could be similar to those of hemp fiber composites.

$E_f = 45.57 \exp [-0.002 (D_f)]$ (IV)

$\sigma_f = 422.03 \exp [-0.018 (D_f)]$ (V)

Mat characterisation

Physical properties of nonwoven cattail mat

The areal density, mat thickness, permeability, and fiber volume fraction (V_f) of nonwoven mats used in manufacturing of composites at three consolidation pressures are tabulated in Table 2. Despite using the same weight to compress the fibers during manufacturing of the mat, the thickness and hence the V_f in the mat varied marginally.

Mat permeability

The out-of-plane permeability of each cattail mat was measured at three different locations and the experimental values are tabulated in Table 2. The mean experimental out of plane permeability values of cattail mat varied from 4.38 x 10^{-11} to 5.97 x 10^{-11} m2. The increase in permeability with decrease in V_f (alternatively increase in % porosity) is evident.

The permeability of cattail non-woven mats in Table 2 is higher than that of nonwoven flax and hemp mats measured using the air medium (Shadhin 2021). The higher permeability values of the cattail mat when compared to those of flax and hemp mats is due to the lower V_f of the cattail mat despite similar areal density. This is believed to be due to longer cattail fibers, which would have resulted in lower level of compaction than hemp or flax fibers during mat manufacturing.

Table 2
Physical properties of nonwoven cattail mat used in manufacturing composites using three consolidation pressures.

Consolidation pressure (kPa)	Areal density of mat (g/m^2), (SD)*	Mat thickness before consolidation (mm)	Fiber volume fraction in mat, V_f %	Out-of-plane Permeability x 10^{-11} (m^2)
101	845	19.3 (0.3)	3.2 (0.06)	5.9 (0.03)
260	921	17 (0.2)	3.9 (0.1)	4.7 (0.2)
560	974	21 (0.2)	3.3 (0.1)	4.9 (0.3)
(SD)* - Standard deviation, N = 3				

Composite characterisation

Effect of consolidation pressure on structure of composite

The measured value of the thickness, density, and fiber volume fraction of cattail composites manufactured at various consolidation pressures, applied during manufacturing, are tabulated in Table 3. The decrease in thickness due to consolidation was maximum at the VARTM pressure of 101 kPa (68.6%). Subsequent consolidation decreased with increase in pressure; 54.3% when the pressure was increased from 101 kPa to 260 kPa and 18.9% when the pressure was increased from 260 to 560 kPa as observed in Table 3.

The fiber volume fraction in the cattail composites increased with increase in consolidation pressure to a maximum at 260 kPa. Instead of increasing further, it marginally decreased when the consolidation pressure was increased further to 560 kPa. This is believed to be due to difference in the compaction behavior of the mats since the three mats used at three compaction temperatures had similar V_f (Table 2). Since the fibers were dropped into the mold manually during manufacturing of the non-woven mat, their arrangement or packing could be different resulting in the observed anomaly in consolidation when the pressure was increased to 560 kPa.

Table 3
Thickness, density, and fiber volume fraction of cattail composites manufactured at various consolidation pressures.

Consolidation pressure (kPa)	Composite thickness after curing (mm)	Density of composite (g/cm^3), (SD)*	Fiber volume fraction in composite, V_f %
101	6 (0.8)	1.19 (0.003)	11.2 (0.4)
260	2.7 (0.04)	1.23 (0.005)	30.4 (0.6)
560	2.2 (0.04)	1.22 (0.002)	26.1 (0.4)
(SD)* - Standard deviation, N = 5			

Mechanical Properties

The tensile stress-strain curves for the cattail fiber reinforced composites, manufactured at different molding pressures, are plotted along with those of the stypol resin are plotted in Fig. 7(b). Also, a representative tensile stress-strain curve for the virgin cattail fiber is shown in Fig. 7(a). It can be inferred that the cattail fiber reinforces the neat resin significantly; however, the level of reinforcement varied with the manufacturing pressures due to variation in V_f with consolidation pressure. The modulus, tensile strength, and failure strain of composites, obtained from these plots, are tabulated in Table 4.

Table 4
Mechanical properties of cattail fiber reinforced composite.

Mat content	Consolidation pressure (kPa)	Longitudinal modulus (GPa) (SD)*	Tensile strength (MPa), (SD)*	Strain at break (%)
100% Cattail	101	4.6 (0.6)	18.6 (3.2)	0.4 (0.1)
100% Cattail	260	7.0 (0.2)	34.0 (3.8)	0.5 (0.1)
100% Cattail	560	6.5 (0.2)	44.1 (2.7)	1.0 (0.1)
(SD)* - Standard deviation, N = 5				

It can be inferred from this Table that the stypol resin is significantly reinforced by the cattail fibers. The magnitude of reinforcement depends on the consolidation pressure due to change in V_f with consolidation pressure. The tensile modulus, strength, and failure strain of cattail composite are plotted as a function of V_f in Figs. 8(a), (b) and (c), respectively.

The tensile modulus increased with pressure until 260 kPa, beyond which it decreased when the pressure was increased to 560 kPa. This is due to increase in V_f from 3.2 to 3.9% in the mat to 11.2% at 101 kPa, which increased to 30.4% at 260 kPa before decreasing to 26.1% at 560 kPa. The reason for this trend in V_f is due to difference in consolidation of the mats, as discussed in the previous section. Linear relation between the modulus and the V_f in Fig. 8(a) clearly establishes the effect of consolidation pressure in increasing the V_f and the modulus of cattail composite. The increase in the modulus and the strength were found statistically significant in two tailed T-test while comparing the values among different groups at different consolidation pressures (Shadhin 2021).

The tensile strength increased with increase in the consolidation pressure (until 260 kPa) during which the V_f also increased. When the pressure was increased further to 560 kPa, the strength increased further from 34 MPa (± 3.8) at 260 kPa to 44.1 MPa (± 2.7), despite lower V_f at 560 kPa as shown in Fig. 8(b and d). Similar trend in the fracture strain is observed in Fig. 8(c). Typically, the failure strain would decrease with increase in the tensile strength. Lower failure strain at 101 kPa and 260 kPa when compared to that at 560 kPa despite lower strength suggests that premature failure, perhaps due to stress concentration, in test specimens manufactured at 101 kPa and 260 kPa could be the reason for the lack of trend in

strength and failure strain with V_f. The relatively highly rough (i.e., ductile) fracture surface of resin area in Fig. 9(c) for 560 kPa when compared to smooth (i.e., brittle) fracture surface of resin area in Figs. 9(a) and 9(b) for 101 kPa and 260 kPa, appear to confirm this interpretation.

At VARTM pressure, the V_f, the modulus and the tensile strength of cattail composites are in similar in magnitude to those of flax and hemp fiber composites (Shadhin 2021), demonstrating the suitability of cattail fibers as reinforcements in Composites.

Future research should consider modification of cattail fiber surface for composites and should study the effect of needle punching on mat and composite properties.

Conclusions

Cattail fibers were successfully extracted, using alkali retting from waste biomass, preformed into a non-woven mat, and used in manufacturing composites using a commonly used unsaturated polyester resin and VARTM used in transportation industries. The extracted fibers exhibited a normal distribution in diameter ($d_{avg.}$ = 32.1 μm) and the modulus and the strength decreased with increase in diameter with average values of 19.1 GPa and 172.3 MPa, respectively. The permeability of cattail mats is higher than those of flax or hemp mats at similar V_f. The modulus and the strength of cattail composite increased with consolidation pressures due to increase in fiber volume fraction (V_f), with maximum values of 7.4 GPa and 48 MPa, demonstrating the utility of cattail fibers from waste biomass as reinforcements. Mechanical properties of cattail fiber and cattail fiber composites are comparable to those of published hemp and flax fibers and their composites.

Abbreviations

VARTM
Vacuum assisted resin transfer molding; PMC:Polymer matrix composite; NFRC:Natural fiber reinforced composites; BFs:Biomass fibers; WBFs:Waste biomass fibers; ASTM:American society for testing and materials; GSM:Gram per square meter; SEM:Scanning electron microscopy.

Declarations

Acknowledgement

Support for this study was provided from Composite Materials and Structures Research Group (CMSRG), department of Mechanical Engineering, and department of Biosystems Engineering, University of Manitoba, Canada.

Funding

The authors received financial support from the University of Manitoba's Research Grant Program (URGP) and the Natural Sciences and Engineering Research Council of Canada (NSERC) to conduct this research.

Availability of data and materials

All data are fully available without restriction.

Authors' contributions

Not Applicable

Ethics approval and consent to participate

No animal or human subjects were used in this work.

Consent for publication

This manuscript does not contain any individual person's data.

Competing interests

The author(s) declared no potential conflicts of interest with respect to the research, authorship, and/or publication of this article.

References

1. Ali A (2013) Surface Modification of Hemp Fiber to Improve Spinning Properties. M.Sc. thesis, University of Manitoba
2. ASTM D1776-04 Standard Practice for Conditioning and Testing Textiles. ASTM International, https://compass-astm-org.uml.idm.oclc.org/download/D1776-04.32339.pdf (2004, accessed 14 March 2021)
3. ASTM D3822-14 (Reapproved 2020) Standard Test Method for Tensile Properties of Single Textile Fibers. ASTM International, https://compass-astm-org.uml.idm.oclc.org/download/D3822D3822M.29232.pdf (2020, accessed 14 March 2021)
4. ASTM D737-18 Standard Test Method for Air Permeability of Textile Fabrics. ASTM International, https://compass-astm-org.uml.idm.oclc.org/download/D737.14434.pdf (2018, accessed 14 March 2021)
5. ASTM D3039-17 Standard Test Method for Tensile Properties of Polymer Matrix Composite Materials. ASTM International, https://compass-astm-org.uml.idm.oclc.org/download/D3039D3039M.20048.pdf (2017, accessed 15 March 2021)
6. ASTM D4892-89 (Reapproved 2004) Standard Test Method for Density of Solid Pitch (Helium Pycnometer Method). ASTM International, https://compass-astm-org.uml.idm.oclc.org/download/D4892-89R04.9974.pdf (2004, accessed 15 March 2021)

7. Canadian Encyclopedia The (n.d.) Wetlands. https://www.thecanadianencyclopedia.ca/en/article/wetlands, retrieved March 18, 2019
8. Campbell FC (2010) Structural composite materials. ASM international Publishing, OH
9. Chakma K (2018) Extraction efficiency, quality, and characterization of Typha latifolia L. fibres for textile applications. M.Sc. thesis, University of Manitoba
10. Davis GC, Bruce DM (1998) Effect of Environmental Relative Humidity and Damage on the Tensile Properties of Flax and Nettle Fibers. Tex Res J 68(9):623–629
11. Fahimian M (2013) Processing-Structure-Property Relationship in Needle-Punched Nonwoven Natural Fibre Mat Composites. Ph.D. Dissertation, University of Manitoba
12. Faruk O, Bledzki AK, Fink HP, Sain M (2012) Biocomposites reinforced with natural fibers: 2000–2010. Prog Polym Sci 37(11):1552–1596
13. Hasan M (2019) Optimization of Typha Fibre Extraction and Properties for Composite Applications Using Desirability Function Analysis. M.Sc. thesis, University of Manitoba
14. Ho MP, Wang H, Lee JH, Ho CK, Lau KT, Leng J, Hui D (2012) Critical factors on manufacturing processes of natural fibre composites. Comp Part B: Eng 43(8):3549–3562
15. Ibrahim I, Sarip S, Bani NA, Ibrahim MH, Hassan MZ (2018) The Weibull probabilities analysis on the single kenaf fiber. AIP Conference Proceedings 1958, 020009. https://doi.org/10.1063/1.5034540
16. Joffea R, Andersons J, Wallstrom L (2003) Strength and adhesion characteristics of elementary flax fibres with different surface treatments. Comp Part A 34:603–612
17. Karnani R, Mohan K, Ramani N (1997) Biofibre-reinforced polypropylene composites. Polym Eng Sci 2:476–483. doi:10.1002/pen.11691
18. Lau KT, Hung PY, Zhu MH, Hui D (2018) Properties of natural fibre composites for structural engineering applications. Comp Part B: Eng 136:222–233
19. Lee CH, Abdan K, Lee SH, Liu M (2019) A Comprehensive Review on Bast Fiber Retting Process for Optimal Performance in Fibers Reinforced Polymer Composites. Adv Mat Sci Eng 2020:27. https://doi.org/10.1155/2020/6074063
20. Li X, Tabil LP, Panigrahi S (2007) Chemical Treatment of Natural Fibre for Use in Natural Fibre Composites: A Review. J Polym Environ 15:25–33
21. Mazumdar S (2001) Composites manufacturing: materials, product, and process engineering. CrC press
22. Miao M, Finn N (2008) Conversion of natural fibres into structural composites. J Tex Eng 54(6):165–177
23. Moudood A, Hall W, Ochsner A, Li H, Rahman A, Francucci G (2019) Effect of Moisture in Flax Fibres on the Quality of their Composites. J Nat Fib. https://doi.org/10.1080/15440478.2017.1414651
24. Mortazavi SM, Moghadam MK (2009) Introduction of a New Vegetable Fibre for Textile Application. J Appl Polym Sci 113:3307–3312. DOI 10.1002/app.30301

25. Morotn WE, Hearle JWS (2008) Physical properties of textile fibres. 4th edition: Woodhouse Publishing Limited and CRC Press, Cornwall, England
26. Nilsson T (2006) Micromechanical Modelling of Natural Fibres for Composite Materials. M.Sc. thesis, Lund University
27. Nishino T, Koichi H, Masaru K, Katsuhiko N, Hiroshi I (2003) Kenaf reinforced biodegradable composite. Comp Sci Tech 9:1281–1286. doi:10.1016/S0266-3538(03)00099-X
28. Oksman K, Lennart W, Lars AB, Romildo DTF (2002) Morphology and mechanical properties of unidirectional sisal–epoxy composites. J Appl Polym Sci 13:2358–2365. doi.org/10.1002/app.10475
29. Peirce FT (1929) A Two-Phase Theory of the Absorption of Water Vapour by Cotton Cellulose. J Tex Inst Trans 20:6. doi:10.1080/19447022908661486. T133-T150.
30. Placet V, Cisse O, Boubakar ML (2012) Influence of environmental relative humidity on the tensile and rotational behaviour of hemp fibres. J Mat Sci 47(7):3435–3446
31. Rahman M, Cicek N, Chakma K (2021) The Optimum Parameters for Fibre Yield (%) and Characterization of Typha latifolia L. Fibres for Textile Applications. Fib Polym. In press
32. Shadhin M (2021) Comparative evaluation of flax, cattail, and hemp fiber composites. Master's thesis, University of Manitoba
33. Shih JG, Finkelstein SA (2008) Range dynamics and invasive tendencies in Typha latifolia and Typha angustifolia in eastern North America derived from herbarium and pollen records. Wetlands 28(1):1–16
34. Stamboulis A, Baillie CA, Peijs T (2001) Effects of environmental conditions on mechanical and physical properties of flax fibres. Comp Part A: Appl Sci Man 32(8):1105–1115
35. Vetayasuporn S (2007) Using Cattails (Typha latifolia as a substrate for Pleurotus ostreatus (Fr.) Kummer cultivation. J Biol Sci 7:218–221
36. Wambua P, Jan I, Ignaas V (2003) Natural fibres: can they replace glass in fibre reinforced plastics? Comp Science Tech 9:1259–1264. doi:10.1016/S0266-3538(03)00096-4
37. Witztum A, Wayne R (2015) Variation in fiber cables in the lacunae of leaves in hybrid swarms of Typha × glauca. Aqua Bot 124:39–44
38. Wróbel K, Magdalena, Magdalena C, Anna K, Magdalena Ż, Jacek K, Lucyna D, Jerzy H, Maciej P, Jan S New biocomposites based on bioplastic flax fibers and biodegradable polymers. Biotech Prog 5(2012):1336–1346. doi:10.1002/btpr.1599
39. Xie Y, Hill CA, Jalaludin Z, Curling SF, Anandjiwala RD, Norton AJ, Newman G (2011) The dynamic water vapour sorption behaviour of natural fibres and kinetic analysis using the parallel exponential kinetics model. J Mat Sci 46(2):479–489
40. Yan L, Nawawi C, Krishnan J (2014) Flax fibre and its composites–A review. Comp Part B: Eng 56:296–317. doi.org/10.1016/j.compositesb.2013.08.014

Figures

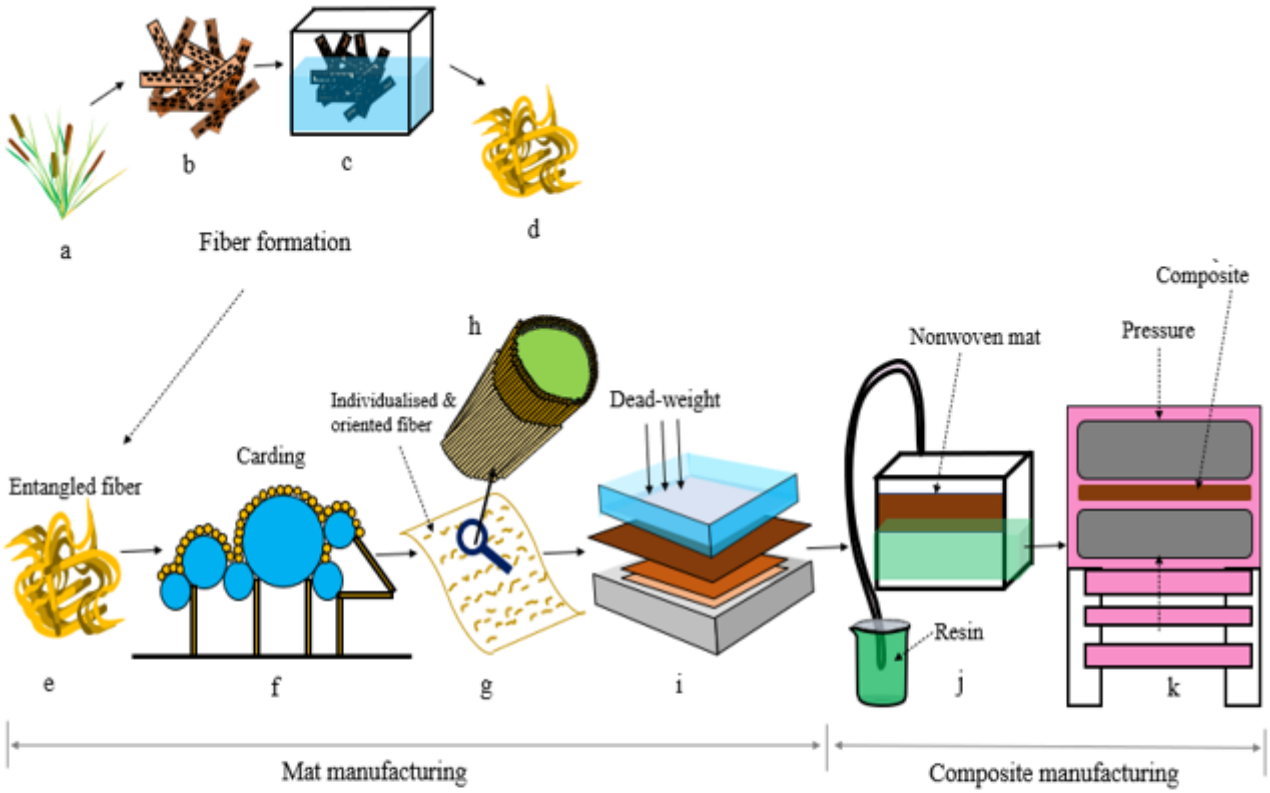

a – green cattail plants

b – 6-10 cm precut cattail leaves

c – alkali retting of cattail (90°C, 4 hrs, 5% KOH

d – extracted cattail fibers after drying

e – entangled fiber bundles fed to carding machine

f - disentangling and combing of fibers via carding process

g - individualised, parallelised, and oriented fiber bundle

h – single cattail fiber

i – dead weight applied on fiber layers placed on template

j- nonwoven mat impregnation by resin in VARTM

k – impregnated mat sandwiched between metal plates, release film, and silicon pad (compression molding)

Figure 1

Schematic diagram for manufacturing compression molded composites using fibers from cattail leaves.

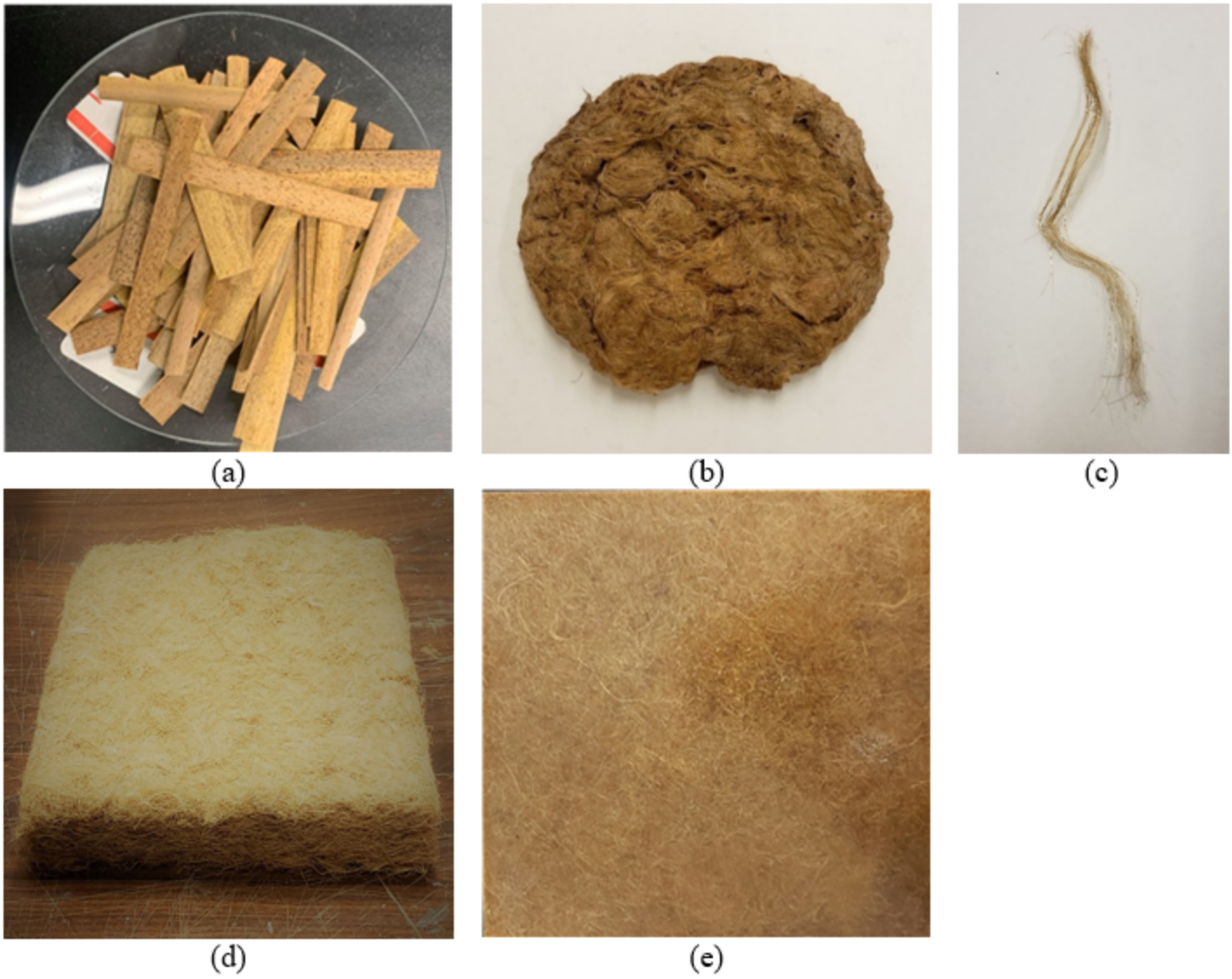

Figure 2

(a) Cattail leaves, (b) Extracted and dried fibers, (c) Individualized fiber, (d) Nonwoven cattail mat, (e) non-woven cattail composite.

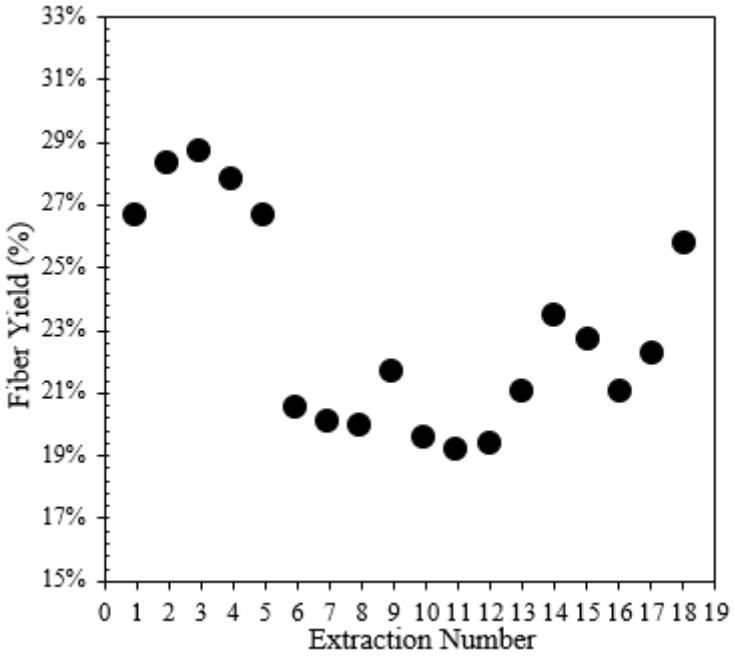

Figure 3

Cattail fiber yield for various extraction runs.

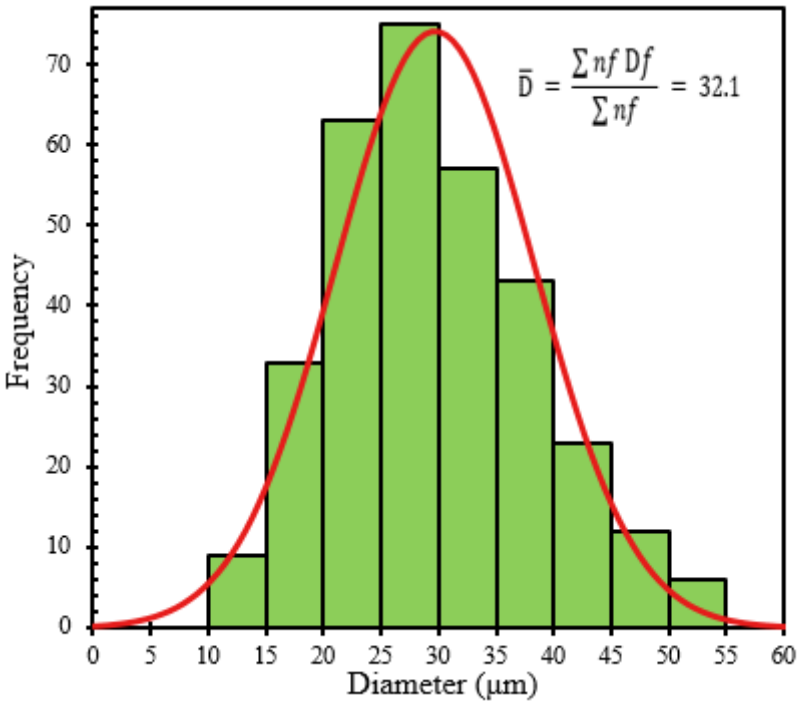

Figure 4

Distribution in (a) length and (b) diameter of cattail fiber.

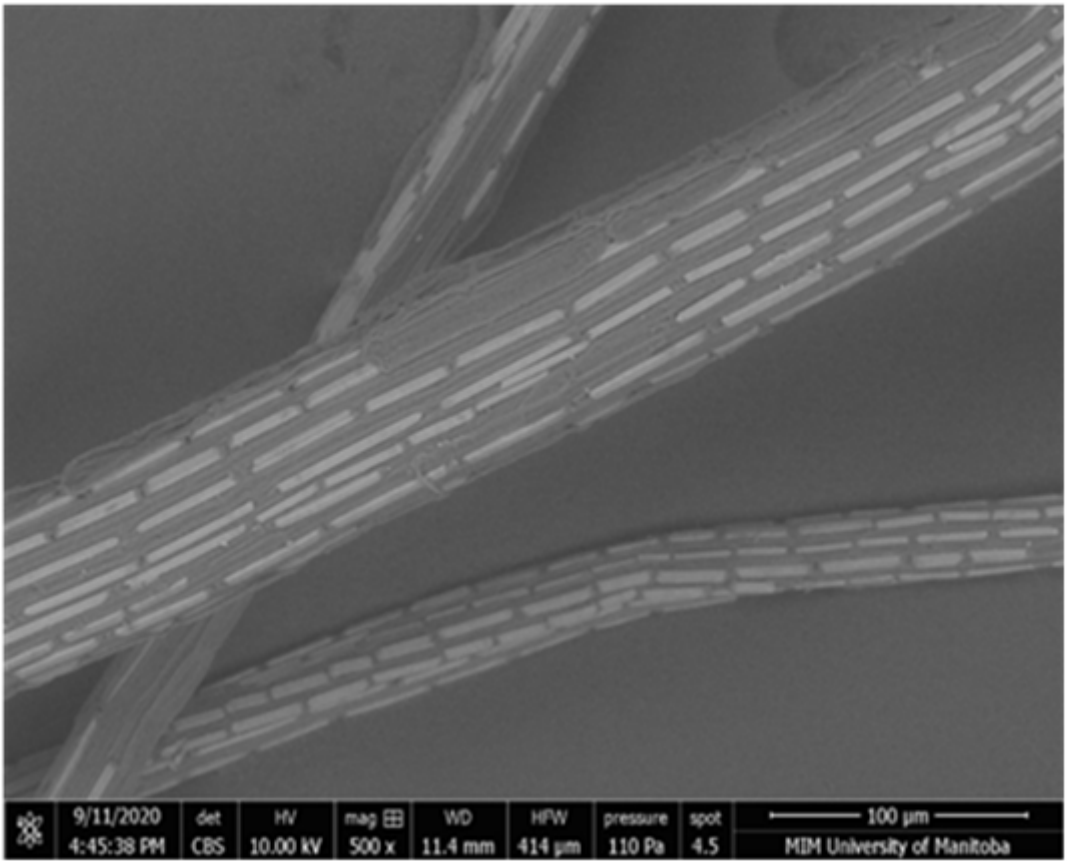

Figure 5

SEM image of cattail fiber.

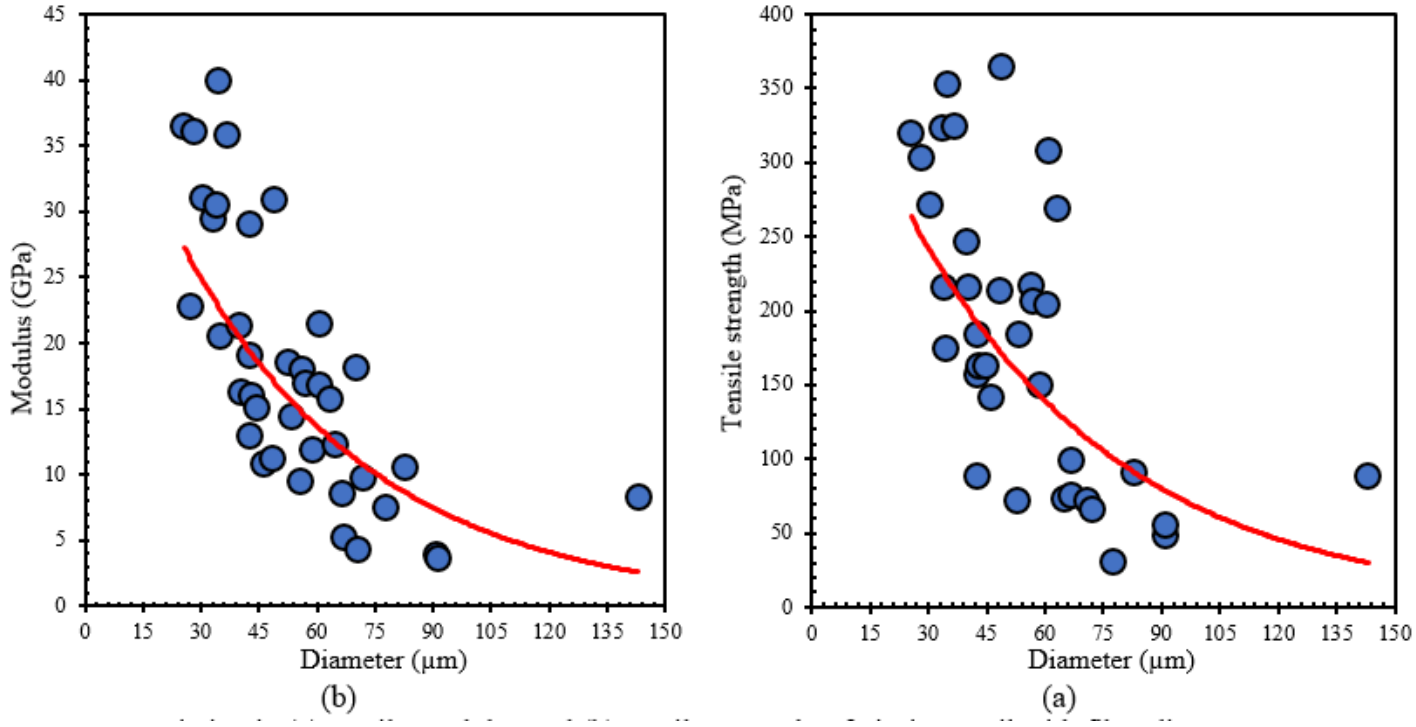

Figure 6

Variation in (a) tensile modulus and (b) tensile strength of virgin cattail with fiber diameter.

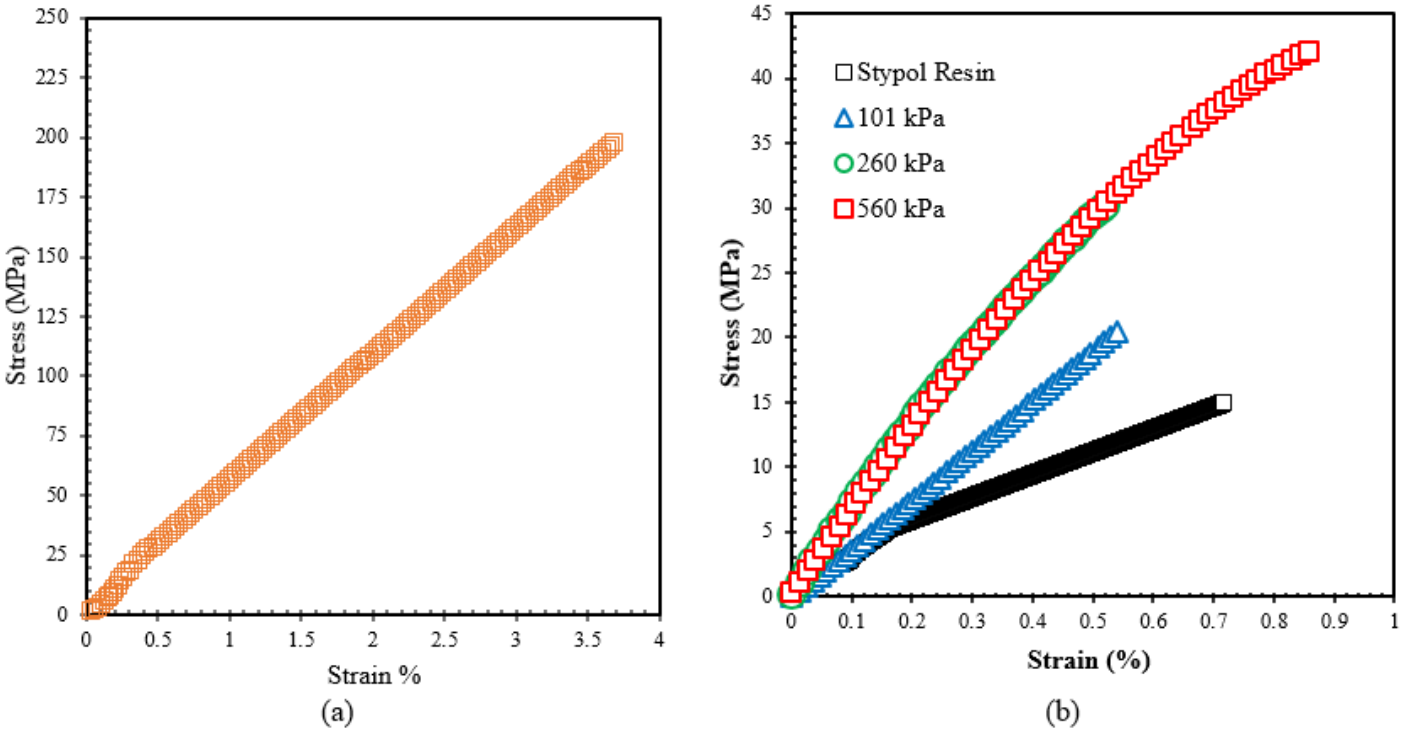

Figure 7

Representative stress-strain curve for (a) cattail fiber and (b) stypol resin and cattail mat composites manufactured at different pressures.

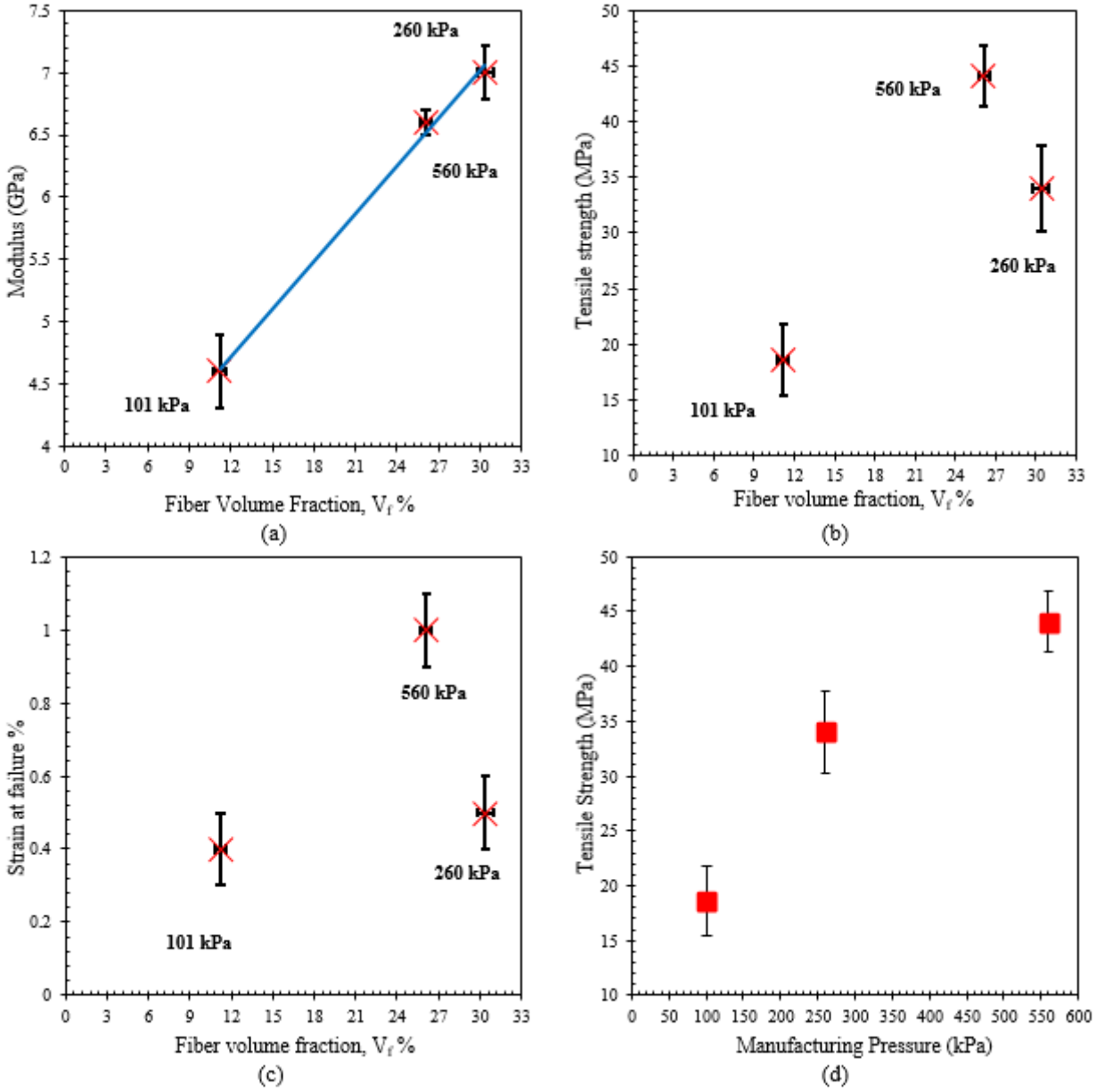

Figure 8

Relationship between (a) tensile modulus and Vf (b) tensile strength and Vf (c) strain at failure and Vf (d) tensile strength and consolidation pressure - for cattail composites.

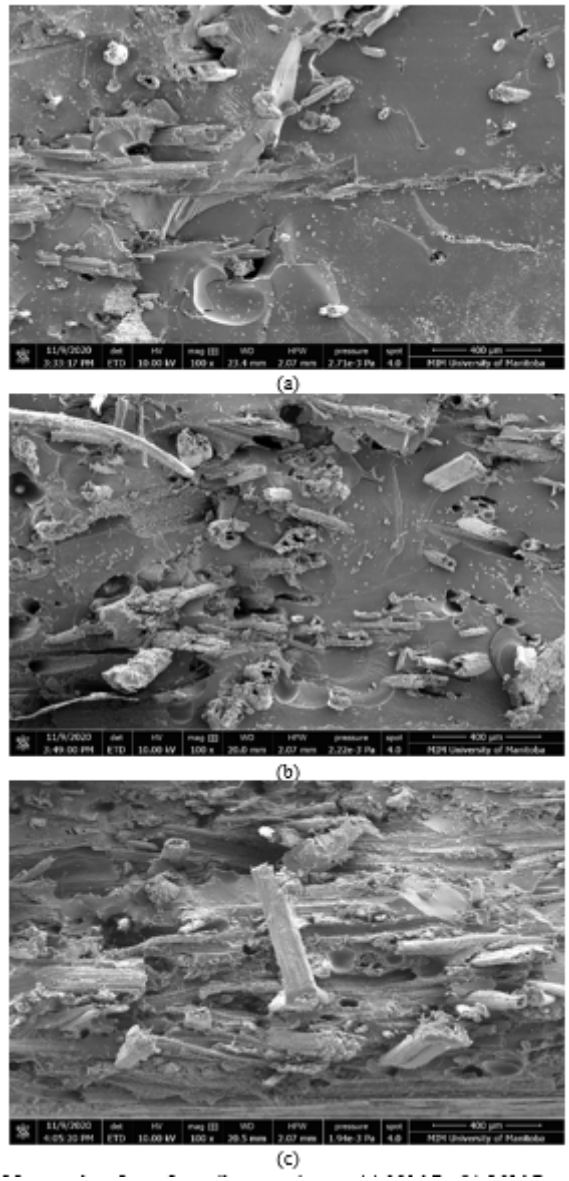

Figure 9

SEM of fractured surface of cattail composite at – (a) 101 kPa (b) 260 kPa and (c) 560 kPa.

Supplementary Files

This is a list of supplementary files associated with this preprint. Click to download.

- GraphicalAbstract..jpg